

Hydro-kinetic approach to relativistic heavy ion collisions

S.V. Akkelin¹, Y. Hama², Iu.A. Karpenko¹, Yu.M. Sinyukov¹

March 8, 2019

Abstract

We develop a combined hydro-kinetic approach which incorporates hydrodynamical expansion of the systems formed in $A+A$ collisions and their dynamical decoupling described by escape probabilities. The method corresponds to a generalized relaxation time (τ_{rel}) approximation for Boltzmann equation applied to inhomogeneous expanding systems; at small τ_{rel} it also allows one to catch the viscous effects in hadronic component - hadron-resonance gas. We demonstrate how the approximation of sudden freeze-out can be obtained within this dynamical picture of continuous emission and find that hypersurfaces, corresponding to sharp freeze-out limit, are momentum dependent. The pion m_T spectra are computed in the developed hydro-kinetic model, and compared with those obtained from ideal hydrodynamics with the Cooper-Frye isothermal prescription. Our results indicate that there does not exist a universal freeze-out temperature for pions with different momenta, and support an earlier decoupling of higher p_T particles. By performing numerical simulations for various initial conditions and equations of state we identify several characteristic features of the bulk QCD matter evolution preferred in view of current analysis of heavy ion collisions at RHIC energies.

¹ *Bogolyubov Institute for Theoretical Physics, 03680 Kiev-143, Metrologichna 14b, Ukraine*

² *Instituto de Física, Universidade de São Paulo, São Paulo, SP, C.P. 66318, 05315-970, Brazil*

PACS: 25.75.-q, 24.10.Nz

Keywords: *relativistic heavy ion collisions, hydro-kinetic model, freeze-out kinetics*

1 Introduction

Hydrodynamic models successfully describe basic features of high energy nuclear collisions at CERN SPS and especially at BNL RHIC (for reviews see, e.g., Refs. [1, 2, 3]), where the utilization of ideal hydrodynamics was supported by theoretical results: it was advocated [4] that the deconfined matter behaves like a perfect liquid. The hydrodynamic approach to $A+A$ collisions implies a very hot and dense strongly interacting matter as the initial state. Such a state is assumed to be formed soon after the collision, then expands hydrodynamically until the stage when the picture of continuous medium is destroyed. Roughly, it happens when the mean free path of particles becomes comparable with the smallest characteristic dimension of the system: its geometrical size or hydrodynamic length. This approach allows one to account for the complicated evolution of the system at pre-confined stage and in the vicinity of the possible phase transitions by means of corresponding equation of state (EoS). Studying the spectra of different particle species versus the initial conditions and EoS, one could get information on thermal partonic stage of the “Little Bang” and further system evolution, which could be also conclusive in the context of discriminating the possible phase transitions.

The problem is, however, whether the predicted momentum spectra, obtained in hydrodynamic models for given initial conditions and EoS, are unambiguous. The point is: these spectra depend not only on the initial conditions but also on the final conditions of hydrodynamic expansion, and one cannot use hydrodynamic equations for infinitely large times since the resulting very small densities destroy the picture of continuous medium of real particles. Evidently, the most simple receipt of spectrum calculation is the Cooper-Frye prescription (CFp) [5] which ignores the post-hydrodynamic (kinetic) stage of matter evolution and assumes that perfect fluid hydrodynamics is valid till some 3D hypersurface, e.g., as was supposed by Landau [6], till isotherm $T \simeq m_\pi$, where sudden transition from local thermal equilibrium to free streaming is assumed.

However, it is known that the particle emission process of fireballs created in high energy heavy ion collisions is gradual in time, therefore fireball emits particles during the whole lifetime of the expanding system. This picture has been discussed in Ref. [7], within a simple ideal hydrodynamics, and also supported by numerical transport codes calculations, e.g., Ref. [8]. It was found in these papers that the transport freeze-out process is similar to evaporation: high- p_T particles freeze out early from the surface, while low- p_T ones decouple later from the system's center. Within CFp the continuous character of emission can be partially taken into account by means of enclosed freeze-out hypersurface with non-space-like sectors.

It is known for a long time that CFp leads to inconsistencies [9, 10], if the freeze-out hypersurface contains the non-space-like sectors, and should be modified to exclude formally negative contributions to the particle number at the corresponding momenta. The simplest prescription is to present the distribution function as a product of a local thermal distribution and the step function like $\theta(p_\mu n^\mu(x))$ [10], $n^\mu n_\mu = \pm 1$, where n^μ is a time-like or space-like outward normal to a freeze-out hypersurface σ . Thereby freeze-out is restricted to those particles for which $p_\mu n^\mu(x)$ is positive. This receipt was used in Ref. [11] to describe particle emission from enclosed freeze-out hypersurface with non-space-like sectors and it was found that a satisfactory description of central $Au+Au$ collisions at RHIC was reached for a physically reasonable set of parameters. The main features of the experimental data were reproduced: in particular, the obtained ratio of the outward to sideward interferometry radii is less than unity and decreases with increasing transverse momenta of pion pairs. Thereby, the results of Ref. [11] clearly indicate that early particle emission off the surface of the hydrodynamically expanding fireball could be essential for proper description of matter evolution in $A+A$ collisions.

However, sharp freeze-out at some 3D hypersurface is a rather rough approximation of the spectrum formation. Results of many studies based on cascade models contradict the idea of sudden freeze-out and demonstrate that in fact particles are emitted from 4D volume during the whole period of the system evolution, and deviations from local equilibrium conditioned by continuous emission should take place (see, e.g., [12]). Moreover, typically, included freeze-out hypersurfaces contain non-space-like parts that lead to problem with energy-momentum conservation law in realistic dynamical models [10]. This concerns also hybrid models [13] where transport model matches hydrodynamics on a such kind of isothermal hypersurface of hadronisation [14]¹. An attempt to introduce 4D continuous emission in hydrodynamic framework has been done in Ref. [7]. This approach was further developed based on Boltzmann equations in Ref. [15] where, in particular, an approximate method that accounts for back reaction of the emission on the fluid

¹ Note that in this hybrid picture the initial conditions for hadronic cascade calculations could be formulated also on some (arbitrary) *space-like* hypersurface where, however, hadronic distributions are deviated from local equilibrium, in particular, because of an opacity effect for hadrons which are created during "mixed" stage of phase transition. This non-equilibrium effect influences seriously the results of hybrid models in its modern form [13].

dynamics was proposed.

The aim of the present work is twofold. First, we develop the formalism of the hydro-kinetic approach and propose approximations for practical calculations. The problem of self-consistency of the method accounting simultaneously both the particle emission and fluid (in general, viscous) dynamics is studied in detail. The special attention is also paid to discussion of the applicability conditions of the Cooper-Frye prescription for sharp freeze-out.

Second, we develop a simple hydro-kinetic model of hadronic emission that describes the evolution and emission of particles from hydrodynamically expanding system undergoing a phase transition. For the sake of simplicity we consider here one type of escaping particles (pions) only and do not take into account, in numerical calculations, the back reaction of the emission on fluid dynamics. We study within such an approach what type of initial conditions, equation of state, etc., are preferred in view of current analysis of heavy ion collisions at RHIC energies.

2 Hydro-kinetic formalism for heavy ion collisions

In Ref. [15] it was proposed to describe the hadronic momentum spectra in $A+A$ collisions, based on the escape function of particles which are gradually liberated from hydrodynamically expanding systems. The escape function, introduced in [7], is calculated within the Boltzmann equations in specific approximation based on hydrodynamic approach. It was shown that such a picture corresponds to relativistic kinetic equation with the relaxation time approximation for the collision term, where the relaxation time tends to infinity, $\tau_{\text{rel}} \rightarrow \infty$, when $t \rightarrow \infty$, indicating a transition to the free streaming regime. For one component system the equation has the form:

$$\frac{p^\mu}{p_0} \frac{\partial f(x, p)}{\partial x^\mu} = - \frac{f(x, p) - f^{\text{leq}}(x, p)}{\tau_{\text{rel}}(x, p)}. \quad (1)$$

Here $f(x, p)$ is the phase-space distribution function, $f^{\text{leq}}(x, p)$ is the local equilibrium distribution with local velocities, temperatures and chemical potentials that should be found from Eq. (1) and the initial $f_0(x, p)$, and $\tau_{\text{rel}}(x, p)$ is the relaxation time (inverse rate of collisions in gases),

$$\tau_{\text{rel}}(x, p) = \frac{p_0 \tau_{\text{rel}}^*(x, p)}{p^\mu u_\mu}. \quad (2)$$

Here $\tau_{\text{rel}}^*(x, p)$ is related to the local fluid rest frame (local rest frame of the energy flow) where the collective 4-velocity is $u_\mu = (1, \mathbf{0})$. The relaxation time depends on the cross-section and is functional of $f^{\text{leq}}(x, p)$.

As it is well known [16, 17], such kind of equations at $\tau_{\text{rel}} \ll \tau_{\text{exp}}$ (inverse of expansion rate) describe in the first approximation the viscosity effects in gases with coefficient of shear viscosity $\eta \propto \tau_{\text{rel}} n T$. Therefore the method explained below catches in first approximation also the viscosity effects in an expanding hadronic gas, characterized by fields of temperatures T and particle densities n . The viscosity effects in the quark-gluon plasma (QGP) evolution cannot be described in this way since strongly interacting QGP is not a gas, but almost ideal liquid [4].

The formal solution of Eq. (1) can be presented in the following form:

$$f(t, \mathbf{r}, p) = f(t_0, \mathbf{r} - \frac{\mathbf{p}}{p_0}(t - t_0), p) \exp \left\{ - \int_{t_0}^t \frac{1}{\tau_{\text{rel}}(s, \mathbf{r} - \frac{\mathbf{p}}{p_0}(t - s), p)} ds \right\} +$$

$$\int_{t_0}^t \frac{f^{\text{leq}}(t', \mathbf{r} - \frac{\mathbf{p}}{p_0}(t-t'), p)}{\tau_{\text{rel}}(t', \mathbf{r} - \frac{\mathbf{p}}{p_0}(t-t'), p)} \exp \left\{ - \int_{t'}^t \frac{1}{\tau_{\text{rel}}(s, \mathbf{r} - \frac{\mathbf{p}}{p_0}(t-s), p)} ds \right\} dt', \quad (3)$$

where $f(t_0, \mathbf{r}, p)$ is the initial distribution at $t = t_0$. The relaxation time τ_{rel}^* as well as the local equilibrium distribution function f^{leq} are functionals of hydrodynamic variables: temperature T , chemical potential μ and collective 4-velocity u_μ . The space-time dependence of the corresponding variables are determined by demanding the local conservation of the energy-momentum with tensor $T^{\mu\nu}(x)$ and, if necessary, net particle number, with current $n^\mu(x)$ (assuming no particle production)

$$\partial_\mu T^{\mu\nu}(x) = 0, \quad (4)$$

$$\partial_\mu n^\mu(x) = 0, \quad (5)$$

where (see, e.g. [17])

$$T^{\mu\nu}(x) = \int \frac{d^3k}{k_0} k^{\mu\nu} f(x, k), \quad (6)$$

$$n^\mu(x) = \int \frac{d^3k}{k_0} k^\mu f(x, k). \quad (7)$$

These conservation laws lead to rather complicated equations for hydrodynamic variables. Noteworthy, that for expanding system the relaxation time $\tau_{\text{rel}}^*(x, p)$ increases with time and, therefore, the deviations from local equilibrium increase too, thereby preventing a use of the widely applied approximate methods based on expansion of the distribution function in the vicinity of the local equilibrium.

Then to solve the kinetic equation (1), in accordance with the conservation laws (4) and (5), we need an approximate method that could be applied even for strong deviations from local equilibrium. It is not our aim here to suggest an exclusive solution of the problem. Rather some arguments are presented below by the example of relativistic one component Boltzmann gas with particle number conservation,

$$f^{\text{leq}}(x, p) = (2\pi)^{-3} \exp \left(- \frac{p^\mu u_\mu + \mu}{T} \right), \quad (8)$$

to show that such a method could be developed based on the following procedure.

To take into account non-equilibrium effects accompanying the particle emission in inhomogeneous violently expanding systems, we utilize the integral representation (3) of kinetic equation (1). Then, performing a partial integration of the second term in Eq. (3) and, assuming that $f(t_0, \mathbf{r}, p) = f^{\text{leq}}(t_0, \mathbf{r}, p)$, one can decompose the distribution function to a local equilibrium part, f^{leq} , and a part describing a deviation from the local equilibrium behavior, g :

$$f = f^{\text{leq}}(x, p) + g(x, p), \quad (9)$$

where

$$g(x, p) = - \int_{t_0}^t \frac{df^{\text{leq}}(t', \mathbf{r} - \frac{\mathbf{p}}{p_0}(t-t'), p)}{dt'} \exp \left\{ - \int_{t'}^t \frac{1}{\tau_{\text{rel}}(s, \mathbf{r} - \frac{\mathbf{p}}{p_0}(t-s), p)} ds \right\} dt'. \quad (10)$$

Note that both functions, $f^{1\text{ eq}}$ and g , are functionals of hydrodynamic variables, g depends also on the relaxation time τ_{rel} that defines the mean time interval between collisions, and τ_{rel} depends in its turn on the distribution function $f^{1\text{ eq}}$ and the cross section. The evolution of the distribution function $f(x, p)$ should satisfy the energy-momentum conservation and, because $T^{\mu\nu}[f] = T^{\mu\nu}[f^{1\text{ eq}} + g] = T^{\mu\nu}[f^{1\text{ eq}}] + T^{\mu\nu}[g]$ for systems where the interaction energy can be neglected, it takes the form of hydrodynamic equations for the perfect fluid with “source”,

$$\partial_\nu T^{\nu\beta}[f^{1\text{ eq}}] = G^\beta[g], \quad (11)$$

where

$$G^\beta[g] = -\partial_\nu T^{\nu\beta}[g]. \quad (12)$$

The equation that takes into account the conservation of particle number has a similar form:

$$\partial_\nu n^\nu[f^{1\text{ eq}}] = S[g], \quad (13)$$

where

$$S[g] = -\partial_\nu n^\nu[g]. \quad (14)$$

To find an approximate solution of Eqs. (11) - (14), one can solve the equations

$$\partial_\nu T^{\nu\mu}[f^{1\text{ eq}}] = 0, \quad (15)$$

$$\partial_\nu n^\nu[f^{1\text{ eq}}] = 0 \quad (16)$$

and, thereby, utilize the hydrodynamic variables in the perfect fluid approximation. Namely, the hydrodynamic variables in this approximation can be used to calculate the deviation from local equilibrium $g(x, p)$ according to (10) and, then, “source” terms $G^\beta[g]$ and $S[g]$ in the right hand side of Eqs. (11) and (13). Then the left hand sides of these equations are functionals of local equilibrium functions and have the simple ideal fluid forms, while the right hand sides associated with a “source” are explicit functions which describe a deviation from the local equilibrium and depend on hydrodynamic variables in the perfect fluid approximation:

$$\partial_\nu T^{\nu\beta}[f^{1\text{ eq}}(T, u_\mu, \mu)] = G^\beta[T_{\text{id}}, u_\mu^{\text{id}}, \mu_{\text{id}}, \tau_{\text{rel}}^{\text{id}}], \quad (17)$$

$$\partial_\nu n^\nu[f^{1\text{ eq}}(T, u_\mu, \mu)] = S[T_{\text{id}}, u_\mu^{\text{id}}, \mu_{\text{id}}, \tau_{\text{rel}}^{\text{id}}], \quad (18)$$

where, for one component Boltzmann gas with elastic collisions only, the relaxation time $\tau_{\text{rel}}^{\text{id}}$ is the inverse of collision rate and has the following form (in co-moving frame):

$$\frac{1}{\tau_{\text{rel}}^{\text{id}*}(x, p)} = \int \frac{d^3k}{(2\pi)^3} \exp\left(-\frac{E_k - \mu_{\text{id}}(x)}{T_{\text{id}}(x)}\right) \sigma(s) \frac{\sqrt{s(s - 4m^2)}}{2E_p E_k}. \quad (19)$$

Here $E_p = \sqrt{\mathbf{p}^2 + m^2}$, $E_k = \sqrt{\mathbf{k}^2 + m^2}$, $s = (p + k)^2$ is the squared c.m. energy of the pair, and $\sigma(s)$ is the corresponding cross section. A solution $(T(x), u_\mu(x), \mu(x))$ of Eqs. (17), (18) accounts for the back reaction of the emission process on hydro evolution and provides us with the hydrodynamic parameters which finally should be used to calculate the locally equilibrated part $f^{1\text{ eq}}(x, p)$ of the complete distribution function $f(x, p)$. Then, the distribution function obtained in this way, $f(x, p) = f^{1\text{ eq}}[T, u_\mu, \mu] + g[T_{\text{id}}, u_\mu^{\text{id}}, \mu_{\text{id}}, \tau_{\text{rel}}^{\text{id}}]$, satisfies the conservation laws, takes into account the non-equilibrium peculiarities of the evolution and is constructed in agreement with the corresponding EoS. Of course, this scheme allows us to make the next iterations in solving Eq. (1). Note also that, since the “source” term in r.h.s. of Eq. (17) is known function, the causality is preserved in this description of dissipative system.

3 Kinetics of the freeze-out in hydro-kinetic approach

The approach developed in the previous Section allows us to study an important problem: under which conditions the Landau/Cooper-Frye prescription (CFp) of sudden freeze-out is valid and how, then, to define the corresponding 3D freeze-out hypersurface. The CFp is traditionally utilized when hydrodynamics is applied to describe the later stage of the matter evolution in $A+A$ collisions, and also is a basic ingredient of various hydro-motivated parameterizations (see, e.g., [11, 18]). Widely used heuristic freeze-out criterion for finding the freeze-out hypersurface of violently expanding system is either comparability of the hydrodynamic rate of expansion with the kinetic rate of collisions [19] or of the mean free path of particles with the geometrical size of the system [6, 20]. While the problem was extensively studied before (see, e.g., [9, 10, 15, 21]), a complete understanding of the conditions allowing the sharp freeze-out approximation (that is sudden transition from local equilibrium to free streaming) and an unambiguous definition of the corresponding freeze-out hypersurface are still absent. The discussion in this Section based on the analytic approximation to momentum spectra could be, in our opinion, useful for understanding the conditions of applicability of the CFp and improvement of it, if necessary.

To proceed, let us consider the particle momentum density at large enough time, when particles in the system stop to interact, $t \rightarrow \infty$:

$$n(t, p) = \int d^3r f(t, \mathbf{r}, p), \quad (20)$$

where the distribution function is given by Eq. (3). Then

$$n(t, p) = \int d^3r' f(t_0, \mathbf{r}', p) \exp \left\{ - \int_{t_0}^t \frac{1}{\tau_{\text{rel}}(s, \mathbf{r}' + \frac{\mathbf{p}}{p_0}(s - t_0), p)} ds \right\} + \int d^3r' \int_{t_0}^t dt' f^{\text{leq}}(t', \mathbf{r}' + \frac{\mathbf{p}}{p_0}(t' - t_0), p) Q(t', \mathbf{r}', p), \quad (21)$$

where

$$Q(t', \mathbf{r}', p) \equiv \frac{1}{\tau_{\text{rel}}(t', \mathbf{r}' + \frac{\mathbf{p}}{p_0}(t' - t_0), p)} \exp \left\{ - \int_{t'}^t \frac{1}{\tau_{\text{rel}}(s, \mathbf{r}' + \frac{\mathbf{p}}{p_0}(s - t_0), p)} ds \right\}. \quad (22)$$

Here, f^{leq} , τ_{rel} are functionals of temperature, hydrodynamic 4-velocity and chemical potential, and these quantities are governed by hydrodynamic equations (11) - (14). Note that

$$Q(t', \mathbf{r}', p) = \frac{d}{dt'} P(t', \mathbf{r}', p), \quad (23)$$

where $P(t', \mathbf{r}', p)$ is connected with the escape probability $\mathbf{P}(t', \mathbf{r}, p)$ for a particle at phase-space point (\mathbf{r}, \mathbf{p}) at the instant t' to leave the system [15], and has the form:

$$P(t', \mathbf{r}', p) \equiv \exp \left\{ - \int_{t'}^t \frac{1}{\tau_{\text{rel}}(s, \mathbf{r}' + \frac{\mathbf{p}}{p_0}(s - t_0), p)} ds \right\} = \mathbf{P}(t', \mathbf{r}' + \frac{\mathbf{p}}{p_0}(t' - t_0), p). \quad (24)$$

The first term in Eq. (21) describes the contribution to the momentum spectrum from particles that are emitted from the very initial time, while the second term accounts for the emission from 4D volume delimited by the initial and final (where particles stop to interact) 3D hypersurfaces, and the integrand is the so called 4D emission function (or emission density)

$$S(t', \mathbf{r}', p) = f^{\text{leq}}(t', \mathbf{r}' + \frac{\mathbf{P}}{p_0}(t' - t_0), p)Q(t', \mathbf{r}', p). \quad (25)$$

In order to have a tractable approach and set up the conditions of validity of CFP, let us assume that at each \mathbf{r}' there is a maximum in t' of the emission function $S(t', \mathbf{r}', p)$ inside the interval $[t_0, t]$, and that the position of the maximum, $t' = t'_\sigma(\mathbf{r}', p)$, is mainly conditioned by $Q(t', \mathbf{r}', p)$. Then corresponding hypersurface $t'_\sigma(\mathbf{r}', p)$ is defined by the conditions

$$\frac{dQ(t', \mathbf{r}', p)}{dt'} \Big|_{t'=t'_\sigma} = 0, \quad (26)$$

$$\frac{d^2Q(t', \mathbf{r}', p)}{dt'^2} \Big|_{t'=t'_\sigma} < 0, \quad (27)$$

and, utilizing Eq. (22), we get

$$\frac{d\tau_{\text{rel}}(t', \mathbf{r}' + \frac{\mathbf{P}}{p_0}(t' - t_0), p) \Big|_{t'=t'_\sigma}}{dt'} = 1, \quad (28)$$

$$\frac{d^2\tau_{\text{rel}}(t', \mathbf{r}' + \frac{\mathbf{P}}{p_0}(t' - t_0), p) \Big|_{t'=t'_\sigma}}{dt'^2} > 0, \quad (29)$$

where d/dt' is the full time derivative.

Let us demonstrate that Eqs. (28), (29) generalize the heuristic freeze-out criterion [19]. According to the latter, the freeze-out happens when

$$\tau_{\text{scat}} \approx \tau_{\text{exp}}, \quad (30)$$

where $\tau_{\text{scat}}(x)$ is the mean time interval between successive scattering events,

$$\tau_{\text{scat}}(x) = \frac{1}{\langle v\sigma \rangle(x)n(x)}, \quad (31)$$

v is the relative velocity between the scattering particles, $n(x)$ is the particle number density and σ is the corresponding total cross section and the sharp brackets mean an average over the local thermal distribution. The inverse hydrodynamic expansion rate $\tau_{\text{exp}}(x)$ is the collective expansion time scale,

$$\tau_{\text{exp}}(x) = - \left(\frac{1}{n(x)} u^\mu \partial_\mu n \right)^{-1} = - \left(\frac{1}{n(x)} \frac{\partial n}{\partial t^*} \right)^{-1}, \quad (32)$$

where t^* is the proper time in the local rest frame of the fluid.

To demonstrate that heuristic freeze-out criterion (30) follows from Eqs. (28) and (29) under certain conditions, we note first that $\tau_{\text{scat}}(x)$ is similar to $\tau_{\text{rel}}^{\text{id}*}$, see Eq. (19). Then, rewriting Eq. (28) in the form

$$\left(\frac{\partial}{\partial t'} + \frac{\mathbf{P}}{p_0} \frac{\partial}{\partial \mathbf{r}'} \right) \tau_{\text{rel}}(t', \mathbf{r}, p) \Big|_{t'=t'_\sigma, \mathbf{r}=\mathbf{r}'+\frac{\mathbf{P}}{p_0}(t'_\sigma-t_0)} = 1, \quad (33)$$

we get from the above equation that

$$-\left(\frac{1}{\tau_{\text{rel}}(t'_\sigma, \mathbf{r}, p)}\right)^{-1} \left(\frac{\partial}{\partial t'} + \frac{\mathbf{p}}{p_0} \frac{\partial}{\partial \mathbf{r}}\right) \left(\frac{1}{\tau_{\text{rel}}(t', \mathbf{r}, p)}\right) \Big|_{t'=t'_\sigma, \mathbf{r}=\mathbf{r}' + \frac{\mathbf{p}}{p_0}(t'_\sigma - t_0)} = \frac{1}{\tau_{\text{rel}}(t'_\sigma, \mathbf{r}, p)} \Big|_{t'=t'_\sigma, \mathbf{r}=\mathbf{r}' + \frac{\mathbf{p}}{p_0}(t'_\sigma - t_0)}. \quad (34)$$

Now, if we turn to the local rest frame of fluid and neglect there the momentum dependence of the above equation, as well as deviations from local equilibrium, we get, accounting for (19) and (31), that the left hand side of Eq. (34) is approximately $-\left(\frac{1}{n} \frac{\partial n}{\partial t'}\right) \Big|_{t'^*=t'_\sigma}$ while the right hand side is $1/\tau_{\text{rel}}^{\text{id}*}(t'_\sigma, \mathbf{r}^*) \approx 1/\tau_{\text{scat}}(t'_\sigma, \mathbf{r}^*)$, recovering thereby the criterion (30) of the freeze-out. One can note, however, that unlike heuristic definition (30) the true freeze-out hypersurface $t'_\sigma(\mathbf{r}', p)$ depends on momentum² and thereby particles of different momenta freeze out on different hypersurfaces. This result has already been observed in [7] in terms of escape probabilities.

Now, to estimate the accuracy of the Cooper-Frye approximation as the one for a real 4D volume emission by that from 3D freeze-out hypersurface, let us expand $f^{\text{leq}}(t', \mathbf{r}' + \frac{\mathbf{p}}{p_0}(t' - t_0), p)$ near points of maximal emission $t' = t'_\sigma$ in the Taylor series. Then, neglecting terms above the first order in $(t' - t'_\sigma)$ and using Eq. (23), we obtain for the particle momentum density (21) the following approximate expression

$$n(t, p) \approx \int d^3 r' f(t_0, \mathbf{r}', p) P(t_0, \mathbf{r}', p) + \int d^3 r' f^{\text{leq}}(t'_\sigma, \mathbf{r}' + \frac{\mathbf{p}}{p_0}(t'_\sigma - t_0), p) (1 - P(t_0, \mathbf{r}', p)) + \int d^3 r' \frac{df^{\text{leq}}(t', \mathbf{r}' + \frac{\mathbf{p}}{p_0}(t' - t_0), p)}{dt'} \Big|_{t'=t'_\sigma} \int_{t_0}^t dt' (t' - t'_\sigma) \frac{d}{dt'} P(t', \mathbf{r}', p). \quad (35)$$

It is convenient to introduce a new variable, namely

$$\mathbf{r} = \mathbf{r}' + \frac{\mathbf{p}}{p_0}(t'_\sigma(\mathbf{r}', p) - t_0). \quad (36)$$

Then

$$\mathbf{r}' = \mathbf{r} - \frac{\mathbf{p}}{p_0}(t_\sigma(\mathbf{r}, p) - t_0), \quad (37)$$

and the corresponding Jacobian is

$$\det \left[\frac{\partial r'_i}{\partial r_j} \right] = 1 - \frac{\mathbf{p}}{p_0} \frac{\partial t_\sigma}{\partial \mathbf{r}}. \quad (38)$$

The particle momentum density $n(t, p)$ acquires the form

$$n(t, p) \approx \int d^3 r \left| 1 - \frac{\mathbf{p}}{p_0} \frac{\partial t_\sigma}{\partial \mathbf{r}} \right| [f(t_0, \mathbf{r} - \frac{\mathbf{p}}{p_0}(t_\sigma - t_0), p) - f^{\text{leq}}(t_\sigma, \mathbf{r}, p)] P(t_0, \mathbf{r} - \frac{\mathbf{p}}{p_0}(t_\sigma - t_0), p) + \int d^3 r \left| 1 - \frac{\mathbf{p}}{p_0} \frac{\partial t_\sigma}{\partial \mathbf{r}} \right| f^{\text{leq}}(t_\sigma, \mathbf{r}, p) \left(1 + \frac{\Delta(\mathbf{r}, p) \frac{d}{dt'} f^{\text{leq}}(t', \mathbf{r} + \frac{\mathbf{p}}{p_0}(t' - t_\sigma), p) \Big|_{t'=t_\sigma}}{f^{\text{leq}}(t_\sigma, \mathbf{r}, p)} \right), \quad (39)$$

²The momentum dependence of freeze-out hypersurface is conditioned by both momentum and spatial dependences of τ_{rel} . Note that the momentum dependence of the relaxation time was explicitly demonstrated recently in Ref. [22] based on the numerical results of parton cascade simulations.

where

$$\Delta(\mathbf{r}, p) \equiv \int_{t_0}^{t \rightarrow \infty} dt' (t' - t_\sigma) \frac{d}{dt'} P(t', \mathbf{r} - \frac{\mathbf{p}}{p_0} (t_\sigma(\mathbf{r}, p) - t_0), p) \quad (40)$$

characterizes the width in t' of the emission function (see (23), (25)). Evidently, the approximation used to obtain Eq. (39) can be justified if the variance of $f^{1 \text{ eq}}$ within the width of the emission function, Δ , is relatively small as compared to the value of $f^{1 \text{ eq}}$ at the maximum of the emission, $t' = t_\sigma$, for any \mathbf{r} and \mathbf{p} ,

$$\left| \frac{\Delta \frac{d}{dt'} f^{1 \text{ eq}}(t', \mathbf{r} + \frac{\mathbf{p}}{p_0} (t' - t_\sigma), p) |_{t'=t_\sigma}}{f^{1 \text{ eq}}(t_\sigma, \mathbf{r}, p)} \right| \approx \left| \frac{f^{1 \text{ eq}}(t_\sigma + \Delta, \mathbf{r} + \frac{\mathbf{p}}{p_0} \Delta, p) - f^{1 \text{ eq}}(t_\sigma, \mathbf{r}, p)}{f^{1 \text{ eq}}(t_\sigma, \mathbf{r}, p)} \right| \ll 1. \quad (41)$$

One can see from Eq. (39) that in the general case with non zero thickness of the emission layer, $\Delta \neq 0$, the emission density (25) cannot be approximated by means of the local equilibrium distribution function $f^{1 \text{ eq}}$ smeared by a (proper) time factor $\exp(-(\tau - \tau_0)^2 / \delta\tau^2)$ with constant τ_0 and $\delta\tau^2$. Such an ansatz cannot be used in place of the proper emission function as it is often utilized in hydro-inspired parameterizations (see, e.g., [18]) to take into account the gradual character of freeze-out process in heavy ion collisions. In fact, parameters τ_0 and $\delta\tau^2$ should be dependent at least on the spacial coordinates, as it is explained in detail in Refs. [11, 15]. Equation (39) demonstrates that they depend on particle momentum as well and that the emission is not locally isotropic.

The thickness $\Delta \rightarrow 0$, when the escape probability $\mathbf{P}(t', \mathbf{r} + \frac{\mathbf{p}}{p_0} (t' - t_\sigma), p) = P(t', \mathbf{r} - \frac{\mathbf{p}}{p_0} (t_\sigma - t_0), p) \rightarrow \Theta(t' - t_\sigma)$, as it follows from (40). Then particles can escape only in the outward direction from the sharp border $t_\sigma(\mathbf{r})$ between the local equilibrium region, where the relaxation time is equal to zero, and the free streaming one, where the relaxation time is equal to infinity, and so, this hypersurface is the freeze-out hypersurface for particle momentum spectra. The local outward normal $n_\mu(\mathbf{r}, p)$,

$$n_\mu = \pm \frac{(1, -\frac{dt_\sigma}{d\mathbf{r}})}{\sqrt{|1 - (\frac{\partial t_\sigma}{\partial \mathbf{r}})^2|}}, \quad (42)$$

to 3D hypersurface $t_\sigma \equiv t_\sigma(\mathbf{r}, p)$ can be time-like ($n_\mu n^\mu = 1$) or space-like ($n_\mu n^\mu = -1$). The pieces of the hypersurface corresponding to time-like normal are space-like ($ds^2 = dt(\mathbf{r})^2 - d\mathbf{r}^2 < 0$) and sign in front of Eq. (42) should be then “+”, while it can be either “+” or “-” for non-space-like sectors (there are $d\mathbf{r}$ on this part of hypersurface such that $ds^2 = dt(\mathbf{r})^2 - d\mathbf{r}^2 > 0$).

Inasmuch as hypersurface $t_\sigma(\mathbf{r}, p)$ corresponds to the maximum of particle emission with momentum \mathbf{p} , these particles cannot be emitted from this hypersurface inward the system on the conditions that $\Delta \rightarrow 0$, because for particles moving inward $S = f^{l.eq} \cdot Q \rightarrow 0$. Hence $p^\mu n_\mu(p) > 0$ across the hypersurface where fairly sharp maximum of emission of particles with momentum \mathbf{p} is situated, and $p^\mu n_\mu(p) > 0$ is a necessary condition for $t_\sigma(\mathbf{r}, p)$ to be a true hypersurface of maximum of emission. It means that hypersurfaces of maximal emission for a given momentum \mathbf{p} may be open in space-time, not enclosing the high-density matter, and different for different \mathbf{p} . To get CFp one should suppose that the integral in (39) over d^3r in the regions where Δ is not small is negligible.

Finally, the conditions for the utilization of Landau/Cooper-Frye approximation of sudden freeze-out are the following:

i) For each momentum \mathbf{p} , there is a region of \mathbf{r} where the emission function (25) has a sharp maximum with temporal width $\Delta(\mathbf{r}, p)$. In accordance with the condition (41), this width should be smaller than the corresponding temporal homogeneity length $\Lambda(\mathbf{r}, p)$ defined from the equation

$$\left| \frac{f^{1\text{ eq}}(t_\sigma + \Lambda, \mathbf{r} + \frac{\mathbf{p}}{p_0}\Lambda, p) - f^{1\text{ eq}}(t_\sigma, \mathbf{r}, p)}{f^{1\text{ eq}}(t_\sigma, \mathbf{r}, p)} \right| \approx 1, \quad (43)$$

i.e., $\Delta \ll \Lambda$.

ii) The escape probabilities $P(t_0, \mathbf{r} + \frac{\mathbf{p}}{p_0}(t_0 - t_\sigma(\mathbf{r}, p)), p) = P(t_0, \mathbf{r} - \frac{\mathbf{p}}{p_0}(t_\sigma(\mathbf{r}, p) - t_0), p)$ for particles to be liberated just from the initial hypersurface t_0 are small almost in the whole spacial region (except maybe peripheral points) and so, one can neglect the first integral in Eq. (39).

iii) Integration in the region of \mathbf{r} where the condition $\Delta \ll \Lambda$ is violated gives relatively small contribution to the particle momentum density. In other words, the space regions where for fixed momentum \mathbf{p} either there is no good maximum of the emission function or phase-space density changes very rapidly are not essential for final momentum distribution. Note, that this condition is most questionable and have to be checked in realistic dynamical approaches for freeze-out, like hydro-kinetics, or transport models with appropriate initial conditions for hadronic phase.

If all points i) - iii) are satisfied, then Eq. (39) can be written in the well known Cooper-Frye form [5]

$$p^0 n(t \rightarrow \infty, p) = \int_{\sigma(p)} d\sigma_\mu p^\mu f^{1\text{ eq}}(x, p), \quad (44)$$

where

$$d\sigma_\mu p^\mu = d^3r \left(p_0 - \mathbf{p} \frac{\partial t_\sigma}{\partial \mathbf{r}} \right). \quad (45)$$

Noteworthy that the freeze-out hypersurface depends on momentum \mathbf{p} and does not necessarily enclose the dense matter (we also will demonstrate it below by numerical calculations). Everywhere on this hypersurface $(p_0 - \mathbf{p} \frac{\partial t_\sigma(\mathbf{r}, p)}{\partial \mathbf{r}}) > 0$, as discussed before. In other words, the momentum dependence of the freeze-out hypersurface, defined by Eqs. (28) and (29), naturally restricts the freeze-out to those particles for which $p^\mu n_\mu(\mathbf{r}, p)$ is positive. Therefore, there are no negative contributions to the particle momentum density from non-space-like sectors of the freeze-out hypersurface, that is a well known shortcoming of Cooper-Frye prescription [9, 10]; the negative contributions could appear only as a result of utilization of improper freeze-out hypersurface that roughly ignores its momentum dependence and so is common for all \mathbf{p} .

4 Pionic emission in specific hydro-kinetic models

In this Section we present and discuss the results of numerical calculations obtained in a few concrete realizations of hydro-kinetic model (HKM). For the sake of simplicity we consider emission of only one particle species (negative pions, π^-) from the expanding fireball. Also we employ here the

ideal fluid approximation for hydrodynamic variables in integral representation (3) to calculate the emission densities and momentum spectra of pions. This approximation results in a little (less than 10% for our calculations) violation of the conservation laws. We describe, in all simulations, the locally equilibrated state of hadrons by relativistic Boltzmann distributions.

The numerical results presented in this Section were obtained on the basis of our original numerical 3D ideal hydro code that was developed based on relativistic Godunov-type HLLC algorithm, described in details in Ref. [23]. We use Bjorken coordinates [24] $\tau = \sqrt{t^2 - z^2}$, $\eta = \tanh^{-1}(z/t)$, instead of Cartesian ones, the corresponding transformation of hydrodynamic equations and conservative variables are described e.g. in Refs. [2, 25]. Second order of accuracy in time of this algorithm is achieved by using the predictor-corrector scheme. To achieve second order of accuracy in space we apply a linear distribution of conservative variables inside each fluid cell. Having determined the evolution in ideal fluid approximation, we proceed in calculating the emission densities using numerical (tabulated) space-time dependencies of collective velocities and thermodynamic quantities. A 8- and 16-point Gaussian quadrature method implemented in ROOT [26] are used to calculate the escape probability for each space-time position and particle momentum. To calculate the resulting 4D integrals for particle spectra we use Monte-Carlo method and check convergence of the results with increasing number of sampling points. We use ROOT for the results output also.

First, we present our results on specific toy-HKM that describes expanding one component relativistic ideal Boltzmann gas ($p = nT$) of π^- with presumed conservation of particle number to demonstrate that our hydro-kinetic approach agrees with the main features of particle emission in mid-rapidity region of relativistic heavy ion collisions, known from results of many transport code simulations. We also compare the particle momentum spectra from HKM with ones obtained by means of Cooper-Frye prescription with standard isothermal freeze-out hypersurface.

We assume the following Bjorken-type initial conditions at $\tau_i = 1$ fm/c for HKM calculations: initial longitudinal flow $v_L = z/t$ without transverse collective expansion, ideal Boltzmann gas of π^- in chemical (local) equilibrium as the initial particle distribution, boost-invariance of the system in the longitudinal direction and cylindrical symmetry with Woods-Saxon initial energy density profile in the transverse plane,

$$\epsilon(\tau_i, r_T) = \frac{\epsilon_0}{\exp\left(\frac{r_T - R_T}{\delta}\right) + 1}, \quad (46)$$

where $R_T = 7.3$ fm, $\delta = 0.67$ fm are associated with the density profile of Au nucleus, and the maximal energy density in the center of the system, $\epsilon_0 = 0.4$ GeV/fm³, corresponding to the temperature $T \approx 320$ MeV of chemically equilibrated pions. To find the momentum spectra in the HKM, the relaxation time $\tau_{\text{rel}} = p_0 \tau_{\text{rel}}^* / p^\mu u_\mu$ needs to be specified. For this aim we utilize the expression given by Eq. (19) that represents the rate of binary collisions for one component Boltzmann gas. As for the cross section, we carry out calculations for two distinct (artificial) values: $\sigma = 40$ mb and $\sigma = 400$ mb. We performed ideal hydro calculations till $\tau_f = 30$ fm/c when the system becomes very rarefied, therefore the interactions are nearly ceased and momentum spectra are almost frozen. The values of $u_\mu(x)$, $T(x)$ and $\mu(x)$ near mid-rapidity, $\eta \approx 0$, are used then to calculate the emission function $S(t', \mathbf{r}', p)$, Eq. (25), and, utilizing Eqs. (21) and (22) to evaluate the momentum spectra at hypersurface $\tau = \tau_f$. Note that the transformation of Eqs. (21) and (22) for evolution parameter τ instead of t with corresponding substitution for the initial conditions can be easily done in a straightforward manner.

The results for the pion emission density integrated over the transverse momenta $\mathbf{p}_T = (p_T \cos \phi, p_T \sin \phi)$ at zero longitudinal momentum, $p_L = 0$,

$$\langle S(x) \rangle_{p_T, \phi} \equiv \int S(x, p) d^2 p_T, \quad (47)$$

as a function of transverse radius r_T and Bjorken proper time τ are shown in Figs. 1 and 2 for $\sigma = 40$ mb and $\sigma = 400$ mb, respectively. The integrated emission function is multiplied by a “geometric” factor τ , because of kinematics in hyperbolic coordinates: $\tau \cdot S(\tau, r_T)$ is associated with the probability for particles with any transverse momentum to be emitted in the central unit of rapidity within the proper time interval $[\tau, \tau + d\tau]$ and transverse radius $[r_T, r_T + dr_T]$. As one can see in these figures, the maximum of emission is more pronounced and occupies narrower space-time area for larger cross sections than for smaller ones, which is certainly a result of higher medium opacity for higher rate of collisions. Therefore the freeze-out is rather gradual process for the low ($\sigma = 40$ mb) value of cross section in the expanding gas, and one could hardly expect the validity of the Cooper-Frye prescription there. Figures 3 and 4 show the dependence of the emission function S on the angle between the position and momentum vectors at the particle emission point in the transverse plane.

To check the reliability of conventional CFp applied at isotherm $T = T_f \sim m_\pi$ versus hydro-kinetic picture of continuous particle emission, we compared the transverse momentum spectrum of emitted pions in HKM with the one calculated in CFp. We performed an integration of the emission function over a space-time 4-volume till $\tau_f = 30$ fm/c to obtain the momentum spectrum of pions in the HKM. The emission of particles already free at the initial moment τ_i was also accounted for in such a calculation. On the other hand, we utilized CFp for isothermal hypersurface with $T_f = 110$ MeV and locally equilibrated distribution function on it. Such a hypersurface, as well as the velocity and chemical potential distributions on it were extracted from a pure hydrodynamic calculation. The results for m_T -spectra ($m_T = \sqrt{p_T^2 + m^2}$) are presented in Fig. 5. One can see the increase of the effective temperature (inverse slope) in the case of small cross section ($\sigma = 40$ mb) as compared to pure hydrodynamic calculations with Cooper-Frye prescription. This happens because, if the collision rate is small, particles can escape easily from the early stages of the evolution when $T > T_f$ (see Fig. 3). While the transverse collective velocity for particles that escape at higher temperatures $T > T_f$ is smaller than the one for particles which suffer freeze out according to CFp at $T = T_f$, the resulted gain in collective velocity does not lead, typically, to an increase of effective temperature calculated according to ideal hydro equations because of the energy transfer from transverse to longitudinal degrees of freedom. Then the utilization of CFp leads to a noticeable decrease of the inverse slope as compare to the hydro-kinetic result (see Fig. 5). Apparently, the high collision rate that occurs for $\sigma = 400$ mb prevents from early escaping and, consequently, leads to a gradual freeze-out in the rather dilute medium at low temperatures $T < T_f$. The interactions at this stage do not change the momentum spectrum essentially justifying, thereby, the utilization of CFp for $T_f = 110$ MeV isotherm.

Now, let us consider a more sophisticated hydro-kinetic model accounting for some realistic features of the evolution of fireballs created in ultrarelativistic heavy ion collisions. We focus on the mid-rapidity hadronic emission at RHIC energies. Note that resonance decay contributions to pion spectra are not taken into account in the present version of HKM. Therefore, we do not compare our results with experimental data. Our aim here is to study the influence of different types of initial conditions and equations of state on hadronic emission processes. The special attention is paid to the life-time of system that undergoes phase transition, since, as is well known, the long evolution

time is one of the main shortcoming of hydrodynamic and kinetic models aiming to describe quark-gluon plasma (QGP) to hadron gas (HG) transition in relativistic heavy ion collisions: it leads to an overestimate of the the corresponding life-time scale found in HBT analysis [27].

First of all, to solve the relativistic hydrodynamic equations, an equation of state needs to be specified. Because the thermal model analysis of the particle number ratios at RHIC demonstrates almost zero baryon chemical potential [28], we utilize EoS with zero net baryon density. According to lattice QCD calculations, the deconfinement transition at vanishing baryon chemical potential is a rapid crossover rather than a first order phase transition with singularities in the bulk thermodynamic observables [29]. Therefore for the calculations presented here, we use for high temperatures a realistic EoS [30] adjusted to the QCD lattice data with crossover transition at about $T_c \approx 175$ MeV and matched with an ideal chemically equilibrated multi-component hadron resonance gas at $T = T_c$. For temperatures in the interval $T_{\text{ch}} < T < T_c$, $T_{\text{ch}} = 160$ MeV, we utilize EoS [30] of an ideal chemically equilibrated multi-component hadron resonance gas, and for $T < T_{\text{ch}}$ we obtain and utilize EoS of a multi-component [31] hadron resonance gas with chemical composition frozen at $T = T_{\text{ch}}$. The resonance mass spectrum extends over all mesons and baryons with masses below 2.6 GeV [31]; corresponding electronic tables were taken from FASTMC event generator [32]. The value of the chemical freeze-out temperature, $T_{\text{ch}} = 160$ MeV, is chosen because it is near chemical decoupling temperatures [28] extracted from the measured hadron abundance ratios at RHIC.³

Then, to calculate the equations of state $p = p(T, \mu_1, \dots, \mu_n)$, $\epsilon = \epsilon(T, \mu_1, \dots, \mu_n)$ of the chemically frozen ideal hadron resonance gas, one needs to know how chemical potential μ_i of each particle species and energy density depend on temperature when hadron gas, being in initially *known* state (all $T_{\text{ch}}, \epsilon_{\text{ch}}, \mu_{\text{ch}}^i$ are known), expands adiabatically. It can be done in the following way. Firstly, note that the concentration of any particle species "i",

$$\kappa_i = \frac{n_i(T, \mu_i)}{n(T, \mu_1, \dots, \mu_n)}, \quad n = \sum n_i, \quad (48)$$

is fixed by its initial value at T_{ch} and, so,

$$\frac{n_i(T, \mu_i)}{n_j(T, \mu_j)} = \frac{\kappa_i}{\kappa_j} \quad (49)$$

does not change with temperature for $T < T_{\text{ch}}$. Here n_i is the number density of particle species "i" and, in Boltzmann approximation,

$$n_i = \frac{(2j_i + 1)}{2\pi^2} T m_i^2 \exp(\mu_i/T) K_2(m_i/T), \quad (50)$$

where $K_n(u) = \frac{1}{2} \int_{-\infty}^{+\infty} dz \exp[-u \cosh z + nz]$, with $\text{Re } u > 0$, is the modified Bessel function of order n ($n = 0, 1, \dots$). The energy density and pressure of the chemically frozen mixture of ideal Boltzmann gases are

$$\epsilon = n(T, \mu_1, \dots, \mu_n) \sum \kappa_i e_i(T), \quad p = n(T, \mu_1, \dots, \mu_n) T, \quad (51)$$

where

$$e_i \equiv \frac{\epsilon_i}{n_i} = m_i \frac{K_1(m_i/T)}{K_2(m_i/T)} + 3T. \quad (52)$$

³Note to avoid misunderstanding that the decay of resonances during hydrodynamic expansion of hadronic matter agrees with chemical freeze-out concept but could influence on EoS and particle spectra. We neglect here this effect just for simplicity reasons.

Then, taking into account the thermodynamic identity

$$\epsilon + p = sT + \sum \mu_i n_i \quad (53)$$

and, accounting for the constancy of entropy density to particle number density ratio, s/n , during an ideal hydro evolution, we divide the above identity by (nT) and get

$$\sum \kappa_i \left(\frac{e_i(T)}{T} - \frac{e_i(T_{\text{ch}})}{T_{\text{ch}}} \right) = \sum \kappa_i \left(\frac{\mu_i(T)}{T} - \frac{\mu_i(T_{\text{ch}})}{T_{\text{ch}}} \right). \quad (54)$$

Equations (54) and (49), (50) define $\mu_i(T)$ for all particle species “ i ” and, thereby, completely the thermodynamic trajectory (for $T < T_{\text{ch}}$) of the system and all their components: $\epsilon(T), p(T), \mu_i(T)$ in isentropic expansion starting from T_{ch} . Of course, the equations of state of the chemically frozen hadron resonance gas (51) can be reduced now to $p(\epsilon)$ on this *particular* thermodynamic trajectory.

For comparison, we also perform ideal hydro calculations with EoS taken from Ref. [33], where strong first order phase transition is assumed. The corresponding EoS are presented in Figs. 6, 7, 8.

To calculate the pionic emission function and momentum spectra by means of HKM, the rate of collisions needs to be specified. We use the expression for collision rate (in the co-moving system) that accounts for binary collisions of pions with any “ i ” hadronic species,

$$\frac{1}{\tau_{\text{rel}}^{\text{id}*}(x, p)} = \sum \int d^3k \frac{g_i}{(2\pi)^3} \exp\left(-\frac{E_{k,i} - \mu_i(x)}{T(x)}\right) \sigma_i(s) \frac{\sqrt{(s - (m - m_i)^2)(s - (m + m_i)^2)}}{2E_p E_{k,i}}. \quad (55)$$

Here $g_i = (2j_i + 1)$, $E_p = \sqrt{\mathbf{p}^2 + m^2}$, $E_{k,i} = \sqrt{\mathbf{k}^2 + m_i^2}$, $s = (p + k)^2$ is the squared c.m. energy of the pair, and $\sigma_i(s)$ is the total cross section in the corresponding binary collision. For the latter, we utilize Breit-Wigner resonance formula with \sqrt{s} -dependent parametrization of decay widths as in Ref. [34]. All relevant resonance states from [31], used in FASTMC event generator [32] - about 320 different species - are taken into account for calculation of $\sigma_i(s)$. Suppression of bulk pionic emission from very high energy density stage of matter evolution where quark-gluon degrees of freedom are dominated is assured in our approach by abrupt increase of the collision rate (55) that is conditioned by drastic increase of hadronic density at $T \gtrsim T_c$ in Eq. (55). Note, to avoid misunderstanding, that we utilize the relaxation rate (55) to calculate the pionic emission for $T > T_c$ for the sake of simplicity only. In more advanced approach the gradual disappearance of pions and other hadronic degrees of freedom during crossover transition as well as the scattering of pions with quarks, gluons, etc. should be taken into account. Here we just expect that it will lead to the same effect of drastic suppression of the pion emission from the region occupied by QGP.

As for the initial conditions, we firstly perform calculations with Woods-Saxon initial energy density profile (46) in the transverse directions at $\tau_i = 1$ fm/c. The values of parameters we choose for illustrative calculations are $\epsilon_0 = 6$ GeV/fm³, $R_T = 7.3$ fm and $\delta = 0.67$ fm. It results in the initial temperature at the central “plateau” $T = 247$ MeV. These initial conditions at mid-rapidity are similar to the ones used in Ref. [35], where the transverse energy density distribution at $\tau_i = 1$ fm/c was parameterized by a flat region with Gaussian smearing near the edge. The hydro evolution starts at $\tau_i = 1$ fm/c with initial Bjorken flow without transverse velocity ($v_T = 0$), assuming a complete chemical equilibrium at $T > T_{\text{ch}}$ and a chemically frozen evolution below T_{ch} .

The \mathbf{p}_T -integrated pion emission function at mid-rapidity is shown in Fig. 9 for EoS with crossover transition and in Fig. 10 for EoS with strong first order phase transition taken from Ref.

[33]. One can see that the utilization of the EoS with crossover transition leads to a significant decrease of the system life-time because of a more effective acceleration of the system [36] in expansion and, therefore, is more reliable in view of RHIC data indicating a rather short lifetime of the system [27].⁴

Results for non- \mathbf{p}_T -integrated emission function are presented in Fig. 11. They demonstrate the tendency of high- p_T particles to be emitted early from the periphery of the system, whereas low- p_T particles are mostly emitted at the late stage of evolution from the center of the system when the system becomes fairly rarefied because of the expansion. It corresponds to results of Ref. [8], where the same conclusion was drawn based on partonic cascade model calculations. Also we checked the validity of the Cooper-Frye prescription for spectra at two assumed freeze-out hypersurfaces corresponding to the isotherms $T = 110$ MeV and $T = 160$ MeV (see Fig. 12). We find that the effective temperature of the spectrum approximately coincides with the one calculated according to CFp at hypersurfaces $T = 110$ MeV for $p_T \lesssim 1$ GeV and $T = 160$ MeV for $p_T \gtrsim 1$ GeV respectively (see Fig. 13). The spectrum calculated with HKM is concave, as shown in Ref. [7], and demonstrates that utilization of simple \mathbf{p} -independent isothermal CFp for modelling freeze-out for such systems could seriously underestimate the effective temperature of the momentum spectra.

While the system life-time is reduced if EoS with crossover transition is utilized, it could still be too high for reproducing measured values of the HBT radii at RHIC [27]. To study the influence of the initial conditions on the life-time of the system, we perform hydro-kinetic calculations also for Gaussian initial energy density profile, instead of Woods-Saxon one:

$$\epsilon(\tau_i, r_T) = \epsilon_0 \exp\left(-\frac{r_T^2}{R_T^2}\right), \quad (56)$$

where $R_T = 7.3$ fm and normalization constant is $\epsilon_0 = 6.0$ GeV/fm³, so that the total energy in any rapidity slice remains the same as for the Woods-Saxon initial density profile. The transverse-momentum-integrated pion emission function at mid-rapidity is shown in Fig. 14. One can readily note a considerable decrease of the “averaged” emission time due to a faster transverse velocity development because of the initial gradients of density in the whole transverse region and so fast cooling. Next, in addition to the Gaussian energy-density profile, we consider also a (pre-equilibrium) non-zero initial flow in the transverse direction. We set

$$v_T = \tanh\left(0.3 \cdot \frac{r_T}{R_T}\right), \quad (57)$$

and recalculate the normalization of energy density profile, which is $\epsilon_0 = 5.32$ GeV/fm³, so that the total energy of any rapidity slab of matter in mid-rapidity remains the same. The results in the shape of emission function are shown in Fig. 15. One can see that the inclusion of the initial transverse flow leads, as expected, to even faster expansion of matter and, thereby, to more reduction of the mean emission time.

5 Conclusions

We have developed the formalism of the hydro-kinetic model [15] intended for detailed study of the space-time picture of hadronic emission from rapidly expanding fireballs in $A+A$ collisions and,

⁴The same conclusion was reached recently in Ref. [37] based on the analysis of effects of different forms of the sound velocity function on the hydrodynamic evolution of matter created in ultrarelativistic heavy ion collisions.

in this way, to evaluate the observed particle spectra and correlations. The approach developed is consistent with Boltzmann equations and conservation laws, and accounts also for the opacity effects.

The first approximation within this method is done for fireballs undergoing 3D azimuthal symmetric Bjorken-type relativistic expansion. Our calculations show that the widely used phenomenological Landau/Cooper-Frye prescription for freeze-out could be applied, for systems of our interest, only in the limiting case of very large total cross sections among the particles. Then the corresponding freeze-out hypersurface can be found from the developed method, however, obvious dependence of such a hypersurface on the value of particle momentum leads to a modification of CFp even for a sharp freeze-out transition. For realistic cross sections, CFp underestimates the effective temperature of the observed spectra since, during an ideal hydrodynamic expansion, the effective temperature of hadronic transverse spectra is typically decreasing, but particles can escape from the system at early hot stage. The latter process is accounted for by the proposed method.

The recent HBT data at RHIC energies restrict a possible maximal value of the system life-time, that is a serious problem for hydro-kinetic “hybrid” models [13] of matter evolution in relativistic heavy ion collisions. We studied the effects of type/order of phase transition implemented in EoS, as well as of different kinds (Woods-Saxon and Gaussian) of initial transverse profile, on the duration of pionic emission. We found that a realistic EoS, motivated by lattice QCD, produces a faster transverse expansion, reducing thereby the life-time of the system compared with the results based on the EoS with first order phase transition. The most serious reduction of the lifetime is observed for the initial Gaussian density profile, because for this profile there are initial pressure gradients over the whole transverse slice of the system already at the initial moment. Noteworthy, the Gaussian-type energy density profile naturally appears [38] in Color Glass Condensate representation of the initial state of colliding nuclei (for review see, e.g., Ref. [39]) in high energy collisions. Also inclusion of the initial nonzero transverse collective velocity leads to faster expansion of the matter and, thereby, provide an additional decrease of the emission time. We studied the effects of inclusion of such flow in the initial conditions for hydro-kinetic model calculations and found that moderate initial flow developed at the very early pre-thermal stage of the evolution of finite partonic systems into vacuum [40] results in noticeable decrease of the system lifetime. It could indicate a way how the HBT puzzle can be resolved in the hydro-kinetic approach. Further developments of the hydro-kinetic approach and description of the data will be the subject of a follow-up work.

Acknowledgments

We are grateful to M. Laine for providing us with the tabulated equation of state and T. Hirano for his help and advices in hydrodynamic calculations at the initial stage of this work. The work was partially supported by FAPESP (Brazil), under the contract numbers 2004/10619-9 and 2006/55393-3, by the Fundamental Research State Fund of Ukraine, Agreement No. F25/718-2007, and by the Bilateral award DLR (Germany) - MESU (Ukraine) for UKR 06/008 Project, Agreement No. M/26-2008. The research was carried out within the scope of the ERG (GDRE): Heavy ions at ultrarelativistic energies - a European Research Group comprising IN2P3/CNRS, Ecole des Mines de Nantes, Université de Nantes, Warsaw University of Technology, JINR Dubna, ITEP Moscow, and Bogolyubov Institute for Theoretical Physics, NAS of Ukraine.

References

- [1] U. Heinz, J. Phys. G **31**, S717 (2005); arXiv: nucl-th/0512051; P. Huovinen, P.V. Ruuskanen, Ann. Rev. Nucl. Part. Sci. **56**, 163 (2006); T. Hirano, Nucl. Phys. A **774**, 531 (2006).
- [2] Y. Hama, T. Kodama, O. Socolowski Jr., Braz. J. Phys. **35**, 24 (2005).
- [3] C. Nonaka, arXiv:nucl-th/0702082; T. Hirano, arXiv:0704.1699.
- [4] E.V. Shuryak, Prog. Part. Nucl. Phys. **53**, 273 (2004); arXiv:hep-ph/0703208; arXiv:0709.2175; arXiv:0804.1373.
- [5] F. Cooper, G. Frye, Phys. Rev. D **10**, 186 (1974).
- [6] L.D. Landau, Izv. Akad. Nauk SSSR, Ser. Fiz. **17**, 51 (1953).
- [7] F. Grassi, Y. Hama, T. Kodama, Phys. Lett. B **355**, 9 (1995); Z. Phys. C **73**, 153 (1996).
- [8] D. Molnar, M. Gyulassy, Phys. Rev. Lett. **92**, 052301 (2004).
- [9] Yu.M. Sinyukov, Z. Phys. C **43**, 401 (1989).
- [10] K.A. Bugaev, Nucl. Phys. A **606**, 559 (1996).
- [11] M.S. Borysova, Yu.M. Sinyukov, S.V. Akkelin, B. Erasmus, Iu.A. Karpenko, Phys. Rev C **73**, 024903 (2006).
- [12] D. Molnar, M. Gyulassy, Phys. Rev. C **62**, 054907 (2000); L.V. Bravina, K. Tywoniuk, E.E. Zabrodin, J. Phys. G **31**, S989 (2005).
- [13] S.A. Bass, A. Dumitry, Phys. Rev C **61**, 064909 (2000); D. Teaney, J. Lauret, E.V. Shuryak, Phys. Rev. Lett. **86**, 4783 (2001); arXiv: nucl-th/0110037; T. Hirano, U. Heinz, D. Kharzeev, R. Lacey, Y. Nara, Phys. Lett. B **636**, 299 (2006); C. Nonaka, S.A. Bass, Phys. Rev. C **75**, 014902 (2007).
- [14] K.A. Bugaev, Phys. Rev. Lett. **90**, 252301 (2003).
- [15] Yu.M. Sinyukov, S.V. Akkelin, Y. Hama, Phys. Rev. Lett. **89**, 052301 (2002).
- [16] K. Huang, *Statistical Mechanics* (2ed., Wiley, 1987).
- [17] S.R. de Groot, W.A. van Leeuwen, Ch. G. van Weert, *Relativistic Kinetic Theory* (North-Holland Publ. Comp., Amsterdam, 1980).
- [18] F. Retiere, M. Lisa, Phys. Rev. C **70**, 044907 (2004); B. Tomášik, Nucl. Phys. A **749**, 209 (2005); W. Florkowski, Nucl. Phys. A **774**, 179 (2006).
- [19] J. Bondorf, S. Garpman, J. Zimanyi, Nucl. Phys. A **296**, 320 (1978); K.S. Lee, U. Heinz, E. Schnedermann, Z. Phys. C **48**, 525 (1990); F.S. Navarra, M.S. Nemes, U. Ornik, and S. Paiva, Phys. Rev. C **45**, 2552 (1992); E. Schnedermann, U. Heinz, Phys. Rev. C **47**, 1738 (1993).
- [20] Y. Hama and F.S. Navarra, Z. Phys. C **53**, 501 (1992).

- [21] C.M. Hung, E. Shuryak, Phys. Rev. C **57**, 1891 (1998); C. Anderlik, L.P. Csernai, F. Grassi, W. Greiner, Y. Hama, T. Kodama, Z.I. Lazar, V.K. Magas, H. Stöcker, Phys. Rev. C **59**, 3309 (1999); B. Tomášik, U.A. Wiedemann, Phys. Rev. C **68**, 034905 (2003); K.A. Bugaev, Phys. Rev. C **70**, 034903 (2004); S.V. Akkelin, M.S. Borysova, Yu.M. Sinyukov, Acta Phys. Hung. A **22**, 165 (2005); F. Grassi, Braz. J. Phys. **35**, 52 (2005); L.P. Csernai, V.K. Magas, E. Molnar, A. Nyiri, K. Tamosiunas, Eur. Phys. J. A **25**, 65 (2005).
- [22] Z. Xu, C. Greiner, Phys. Rev. C. **76**, 024911 (2007).
- [23] D.H. Rischke, S. Bernard, J.A. Maruhn, Nucl. Phys. A **595**, 346 (1995).
- [24] J.D. Bjorken, Phys. Rev. D **27**, 140 (1983).
- [25] T. Hirano, Phys. Rev. C **65**, 011901 (2001).
- [26] <http://root.cern.ch/>
- [27] U. Heinz, Nucl. Phys. A **721**, 30 (2003); M. Lisa, S. Pratt, R. Soltz, U. Wiedemann, Ann. Rev. Nucl. Part. Sci. **55**, 357 (2005).
- [28] J. Adams *et al.* (STAR Collaboration), Phys. Rev. Lett. **92**, 112301 (2004); Nucl. Phys. A **757**, 102 (2005); A. Andronic, P. Braun-Munzinger, J. Stachel, Nucl. Phys. A **772**, 167 (2006); F. Becattini, J. Cleymans, J. Strumpfer, arXiv:0709.2599.
- [29] F. Karsch, arXiv:hep-lat/0601013; U.M. Heller, arXiv:hep-lat/0610114.
- [30] M. Laine, Y. Schröder, Phys. Rev. D **73**, 085009 (2006).
- [31] W.-M. Yao *et al.* (Particle Data Group), J. Phys. G **33**, 1 (2006).
- [32] N.S. Amelin *et al.*, Phys. Rev. C **77**, 014903 (2008).
- [33] T. Hirano, K. Tsuda, Phys. Rev. C **66**, 054905 (2002).
- [34] S.A. Bass *et al.*, Prog. Part. Nucl. Phys. **41**, 225 (1998).
- [35] K. Morita, S. Muroya, C. Nonaka, T. Hirano, Phys. Rev. C **66**, 054904 (2002).
- [36] Y. Hama, R.P.G. Andrade, F. Grassi, O. Socolowski Jr., T. Kodama, B. Tavares and S.S. Padula, Nucl. Phys. A **774**, 169 (2006).
- [37] M. Chojnacki, W. Florkowski, arXiv:nucl-th/0702030.
- [38] T. Hirano, Y. Nara, Nucl. Phys. A **743**, 305 (2004).
- [39] E. Iancu, R. Venugopalan, in Quark Gluon Plasma 3, eds. R.C. Hwa, X.N. Wang (World Scientific, Singapore, 2004), p.249 [arXiv:hep-ph/0303204]; E. Iancu, A. Leonidov, L. McLerran, arXiv:hep-ph/0202270; R. Venugopalan, Eur. Phys. J. C **43**, 337 (2005).
- [40] Yu.M. Sinyukov, Acta Physica Polonica B **37**, 2926 (2006); M. Gyulassy, Iu.A. Karpenko, A.V. Nazarenko, Yu.M. Sinyukov, Braz. J. Phys. **37**, 1031 (2007).

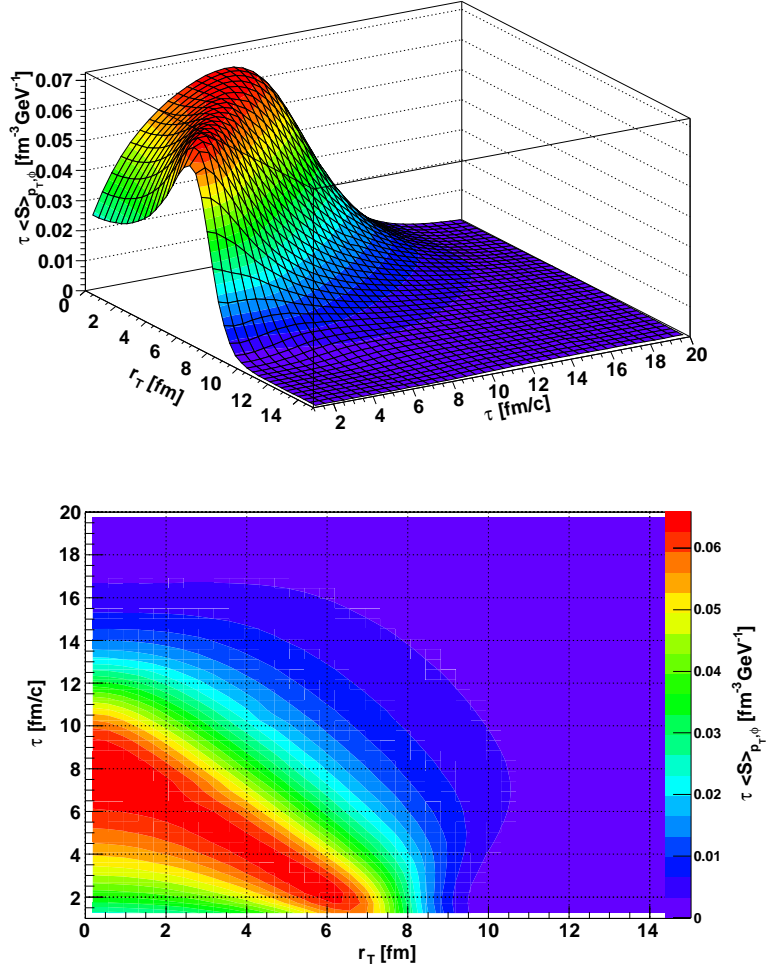


Figure 1: Space-time dependence of the emission function integrated over transverse momenta at $y = 0$, for an expanding gas of pions with cross section 40 mb, initially with longitudinally boost-invariant flow and Woods-Saxon energy density profile in the transverse plane.

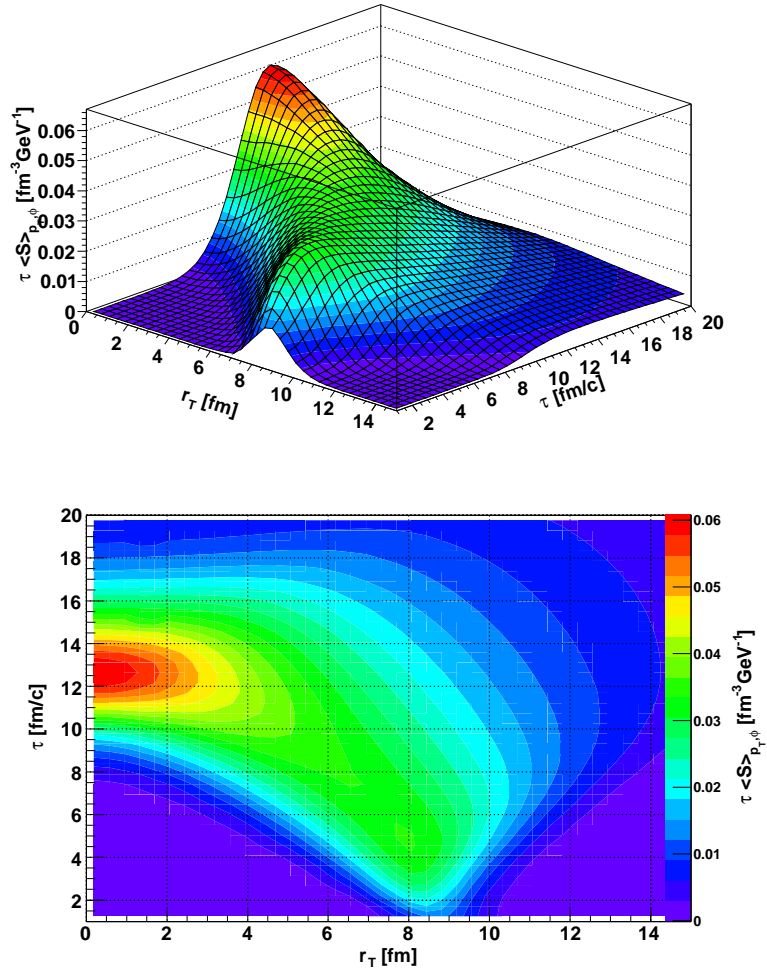


Figure 2: Same as in Fig. 1, with cross section equal to 400 mb.

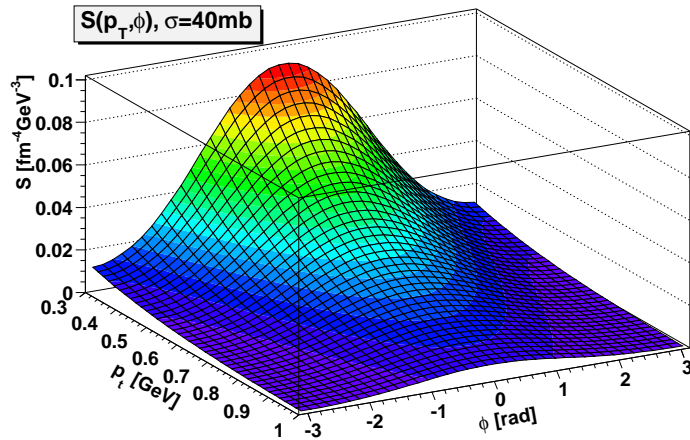


Figure 3: Emission function for an expanding gas of pions with cross section 40 mb at $\tau = 2 \text{ fm}/c$ as function of the angle between the position and transverse momentum vectors of the escaping particle at the distance $r_T = 6 \text{ fm}$ from the axis for different absolute values of transverse momentum.

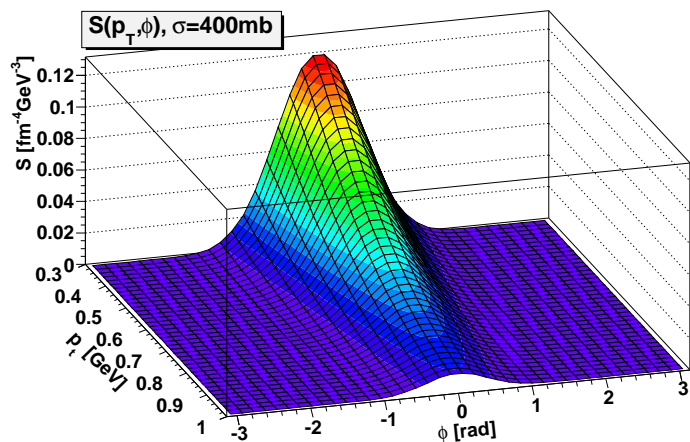


Figure 4: The same as Fig. 3, with cross section 400 mb at $\tau = 4 \text{ fm}/c$ and $r_T = 8 \text{ fm}$.

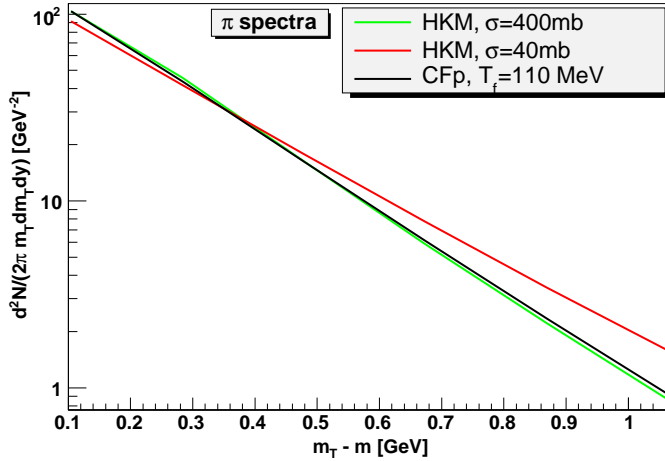


Figure 5: Transverse spectra of pions escaped until $\tau = 30$ fm/c from an expanding fireball calculated in HKM, with cross section 40 mb and 400 mb, compared with the spectrum according to CFp applied to the l.eq. distribution at hypersurface $T_f = 110$ MeV.

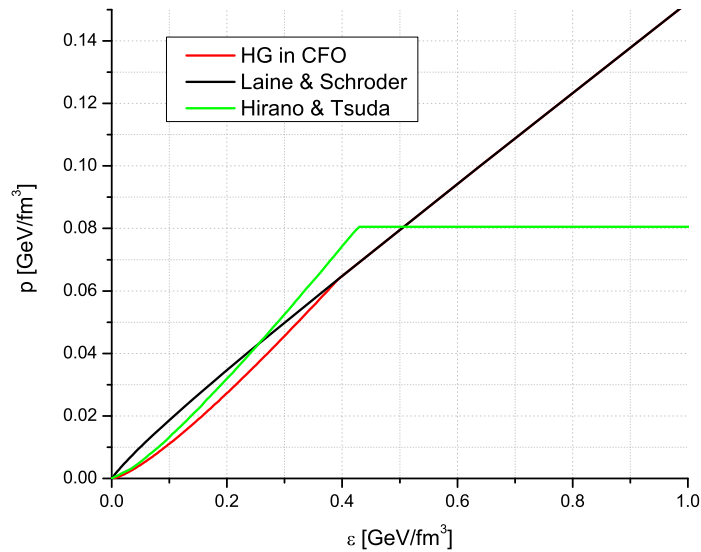


Figure 6: Pressure versus energy density for Laine and Schröder EoS with crossover transition; for Hirano and Tsuda EoS with strong first order phase transition; and for chemically frozen ideal hadron resonance gas.

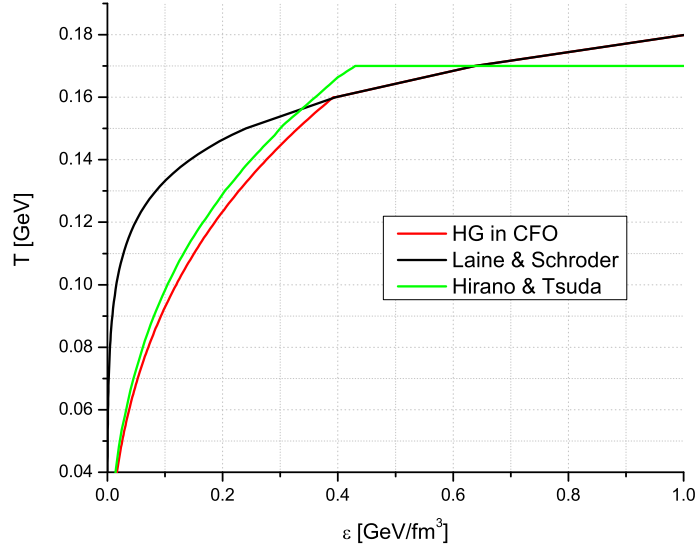


Figure 7: Temperature versus energy density for Laine and Schröder EoS with crossover transition; for Hirano and Tsuda EoS with strong first order phase transition; and for chemically frozen ideal hadron resonance gas.

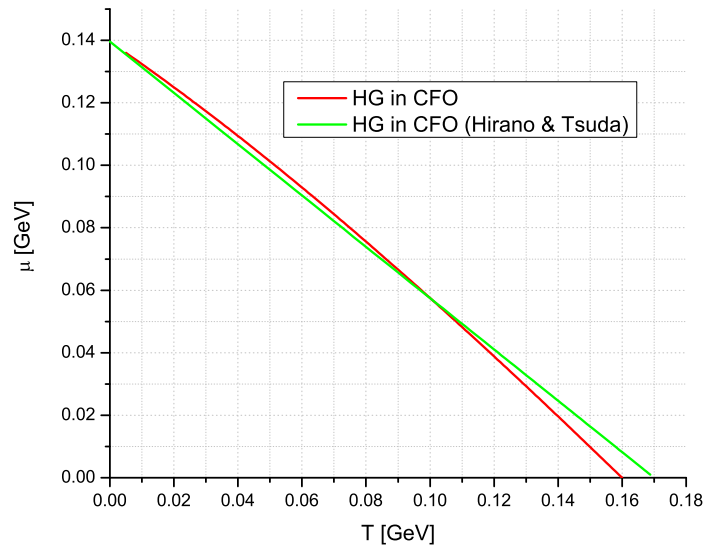


Figure 8: Chemical potential of pions (in the Boltzmann approximation) versus energy density for Laine and Schröder EoS with crossover transition; for Hirano and Tsuda EoS with strong first order phase transition; and for chemically frozen ideal hadron resonance gas.

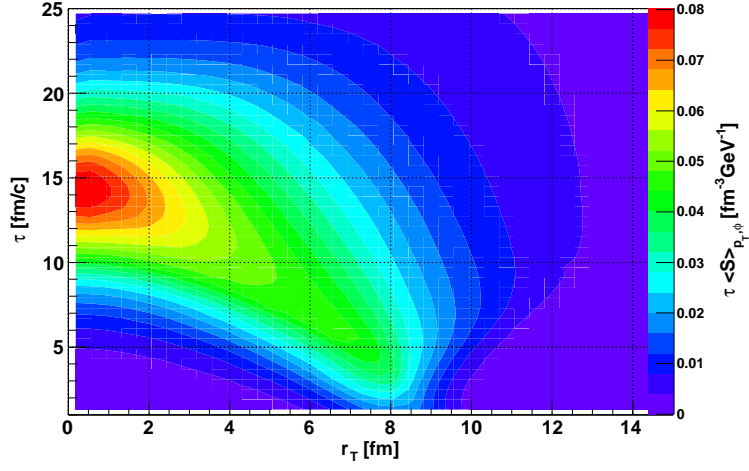


Figure 9: Space-time dependence of the pionic emission function integrated over the transverse momenta for an expanding fireball with *crossover* transition, initially with longitudinally boost-invariant flow and Woods-Saxon energy density profile in the transverse plane.

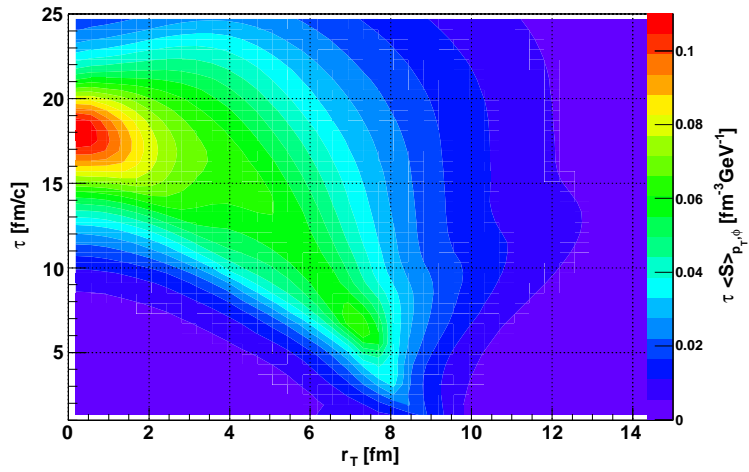


Figure 10: Same as in Fig. 9 with strong *first order phase transition*.

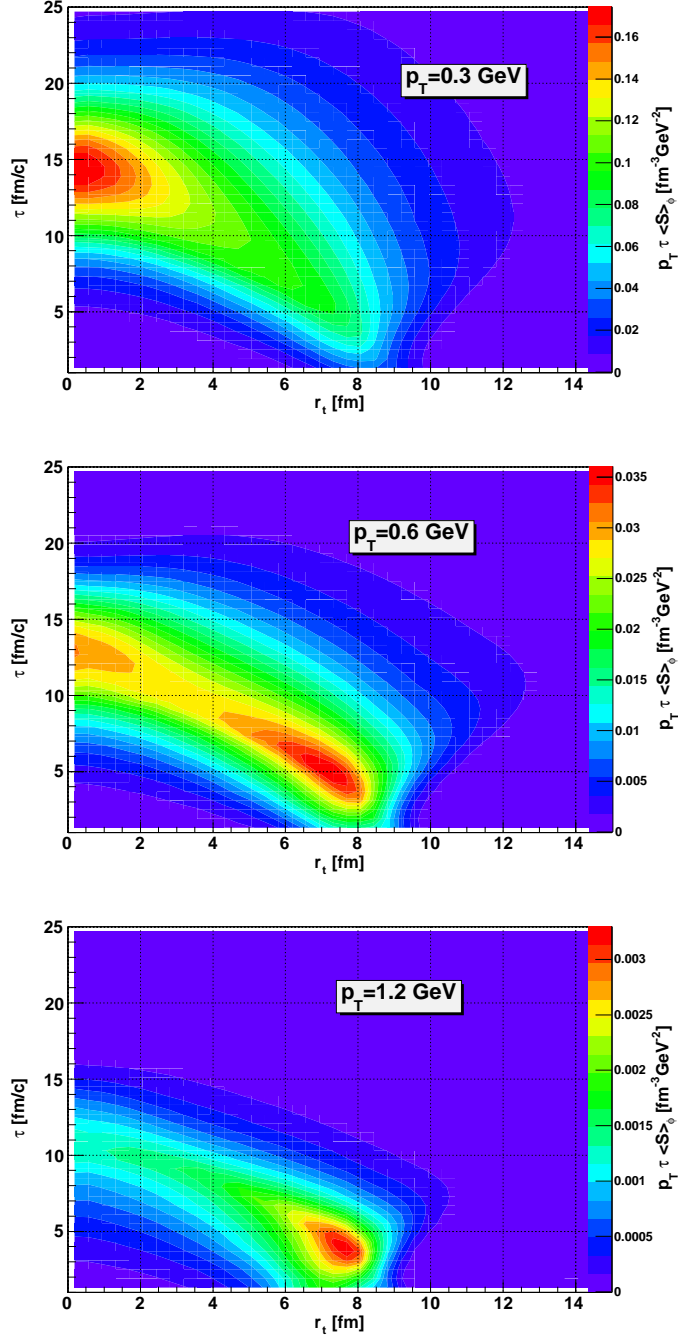


Figure 11: Space-time dependence of the pionic emission function of an expanding fireball with crossover transition and Woods-Saxon initial energy density profile in the transverse plane, at $\phi = 0$ and different values of p_T .

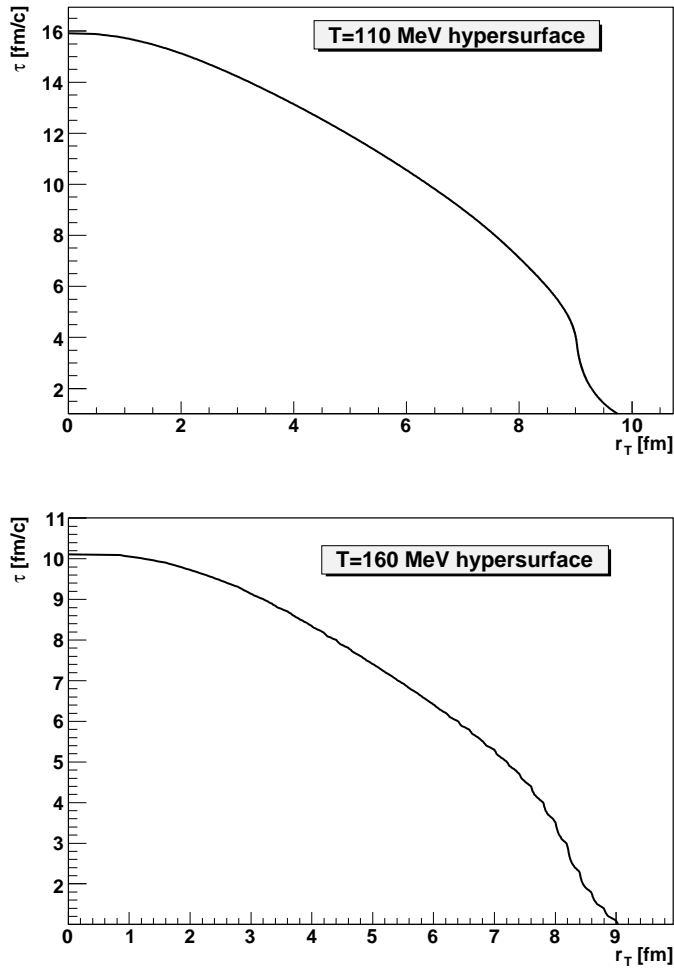


Figure 12: Isothermal hypersurfaces of an expanding fireball with crossover transition and Woods-Saxon initial energy density profile in the transverse plane.

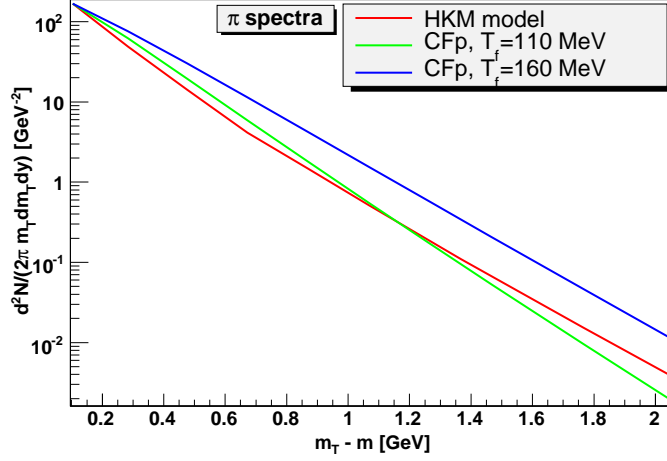


Figure 13: Transverse spectrum of pions escaped until $\tau = 30$ fm/c from an expanding fireball with crossover transition calculated in HKM versus spectra calculated according to CFp applied to the l.eq. distribution at $T_f = 110$ MeV and $T_f = 160$ MeV.

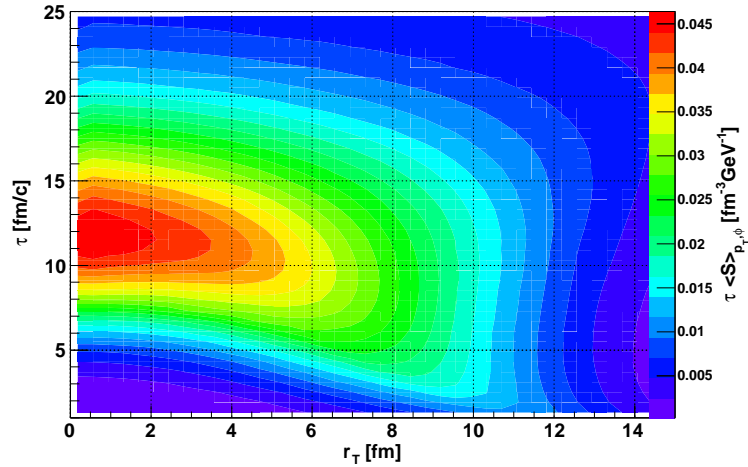


Figure 14: Space-time dependence of the pionic emission function integrated over transverse momenta for an expanding fireball with crossover transition, initially with longitudinally boost-invariant flow and Gaussian energy density profile in the transverse plane.

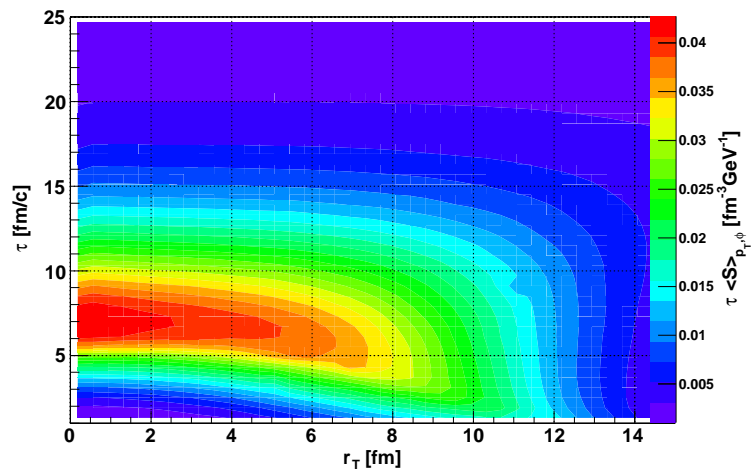


Figure 15: Same as in Fig. 14, but with an initial non-zero transverse flow added.